

RESEARCH OUTPUTS / RÉSULTATS DE RECHERCHE

Nanomorphology of the blue iridescent wings of a giant tropical wasp megascolia procer javanensis (Hymenoptera)

Sarrazin, Michael; Vigneron, Jean-Pol; Welch, Victoria; Rassart, Marie

Published in:

Physical Review. E : Statistical, Nonlinear, and Soft Matter Physics

Publication date:

2008

Document Version

Peer reviewed version

[Link to publication](#)

Citation for pulished version (HARVARD):

Sarrazin, M, Vigneron, J-P, Welch, V & Rassart, M 2008, 'Nanomorphology of the blue iridescent wings of a giant tropical wasp megascolia procer javanensis (Hymenoptera)', *Physical Review. E : Statistical, Nonlinear, and Soft Matter Physics*, vol. 78, pp. 051902-1-5.

General rights

Copyright and moral rights for the publications made accessible in the public portal are retained by the authors and/or other copyright owners and it is a condition of accessing publications that users recognise and abide by the legal requirements associated with these rights.

- Users may download and print one copy of any publication from the public portal for the purpose of private study or research.
- You may not further distribute the material or use it for any profit-making activity or commercial gain
- You may freely distribute the URL identifying the publication in the public portal ?

Take down policy

If you believe that this document breaches copyright please contact us providing details, and we will remove access to the work immediately and investigate your claim.

Nanomorphology of the blue iridescent wings of a giant tropical wasp, *Megascolia procer javanensis* (Hymenoptera)

Michaël Sarrazin,^{1,*} Jean Pol Vigneron,¹ Victoria Welch,¹ and Marie Rassart¹

¹*Laboratoire de Physique du Solide, Facultés Universitaires Notre-Dame de la Paix,
rue de Bruxelles, 61, B-5000 Namur Belgium*

(Dated: February 18, 2013)

The wings of the giant wasp *Megascolia Procer Javanensis* are opaque and iridescent. The origin of the blue-green iridescence is studied in detail, using reflection spectroscopy, scanning electron microscopy and physical modelling. It is shown that the structure responsible for the iridescence is a single homogeneous transparent chitin layer covering the whole surface of each wing. The opacity is essentially due to the presence of melanin in the stratified medium which forms the mechanical core of the wing.

PACS numbers: 42.70.Qs, 42.66.-p, 42.81.-i, 42.81.Qb, 87.19.-j

I. INTRODUCTION

The structural coloration of living organisms is currently receiving much attention [1, 2, 3, 4, 5, 6, 7, 8, 9, 10, 11, 12]. The keys to the visual effects occurring in insects – mainly butterflies and beetles – are being progressively revealed, and the relationship between the cuticle’s nanomorphology and its optical properties is becoming ever more accurate, often with the support of physical modelling and numerical simulations. In a few cases, artificial structures which mimic the natural functions [13] have consolidated our understanding of the colouration mechanisms.

However, some families of insects, though visually appealing, have been studied relatively less. In this work, we report on the analysis of the iridescence of the wings of a giant wasp, *Megascolia procer javanensis* (Betrem & Bradley 1964). Wasps are winged insects which belong to the order Hymenoptera, which also includes ants and bees. Although some wasps have developed social behaviors, the vast majority of the 200,000 species are solitary. Wasps can be found in most regions of both hemispheres. Some are solid black or dark blue, but most of them display conspicuous red, orange, or yellow markings. The wings are opaque or transparent.

Megascolia procer javanensis is a large and robust insect, about 5 cm in length, which belongs to the small family of Scoliidae[14] (see Fig. 1). Organisms in this family have long been observed and studied in relation to their parasitic behaviour, in particular by the French naturalist Jean-Henry Fabre[15]. Members of these Scoliidae are indeed external parasites of Scarabaeid larvae, which means that they are able to sting and thereby paralyze a grub[16], lay an egg on it, and leave it in the soil, so that the developing larva will feed on the grub. The specimen under study here [17, 18] originates from the island of Java. The body of this insect is slightly hairy and the wings show a large number of parallel, longitudinal, wrinkles (see Fig. 2). Moreover, in this particular species, the wings appear black and mostly opaque, with iridescent green to bluish green reflections visible at increasing viewing angles.

The objective of the present paper is to clarify the relationship between the physical structure of the wings, as revealed by scanning electronic microscopy (SEM), and their optical properties. The next sections will show that the wings can be modelled by a thin optical layer probably made of chitin covering a simple chitin/melanin mixture substrate. In order to confirm this interpretation, the experimental spectra of the scattered light will be compared with the results of numerical simulations based on the thin layer model.

II. NANOMORPHOLOGY

Wasp wings are made from a material containing chitin, proteins and melanin, just like the insect’s cuticle. A scanning electron microscope image of a wing, fractured in the direction normal to its surface, reveals that the wings are covered by a thin layer of unknown medium, with a measured average thickness 300 nm (see Fig. 3). A similar uniform layer coverage has also been observed in other insects, such as dragonflies [19]. The bulk of the wing, below the thin layer, is structured as a multilayer, likely to improve mechanical strength. The thickness of the layers varies

*Electronic address: michael.sarrazin@fundp.ac.be

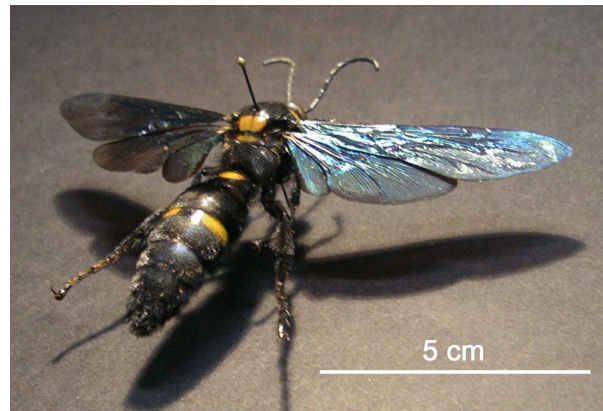


FIG. 1: (Colour online) A collected specimen of male *Megascolia procer javanensis* (Hymenoptera). Note the dark wings of this Scoliid, showing bluish reflections.

along the length of the wing (from about 400 nm to 1 μm), plausibly to provide a variable flexibility. Except for its melanin content, which leads to opacity, this multilayer is probably not directly involved in any blue-green colouring process, because it has a thickness over 400 nm, with an average refractive index above 1.5, making it a Bragg mirror that essentially reflects at wavelengths longer than about $\lambda = 1200 \text{ nm}$: well in the infrared. An harmonic of such a resonance could, in principle, be found in the visible, near 600 nm (orange-red), but this is actually not observed. These findings imply that the multilayer is too lightly contrasted and/or is too absorbent to produce multiple interface scattering.

Another reason to rule out the bulk wing structure as a possible origin of the iridescence is that the layer thickness varies along the wing. If such a structure were to be selectively reflecting, its central colour would vary drastically along the length of the wing and this, again, is not observed. The blue-green hue of the reflection is very uniform on the forewing and hindwing surfaces.

As Fig. 3 shows, the surface of the wing is slightly corrugated, with randomly distributed rounded protrusions. A typical distance between the protrusions' centres is 1.2 μm , which is also their diameter. The protrusions then form a disordered field of touching islands, with an overall thickness of about 80 nm. This structure, again, should not seriously impact upon the colour production, but could be expected to broaden the reflection both in the spectral- and emergence angles- domains.

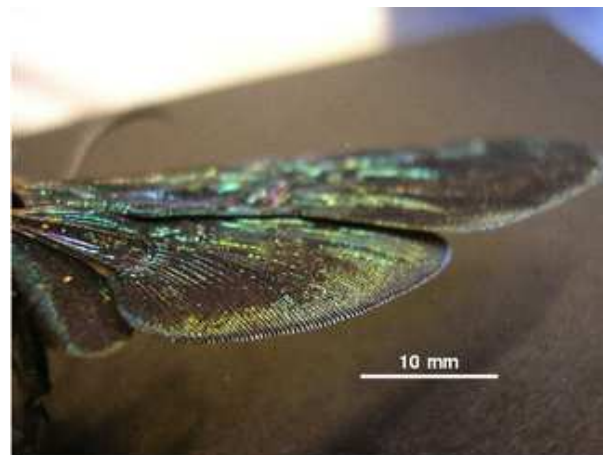


FIG. 2: (Colour online) The wings of *Megascolia procer* are highly sophisticated organs, balancing low inertia, strength and optimized aerodynamics. Note the rippled surface, which produce a wavy cross-section for the bearing membrane.

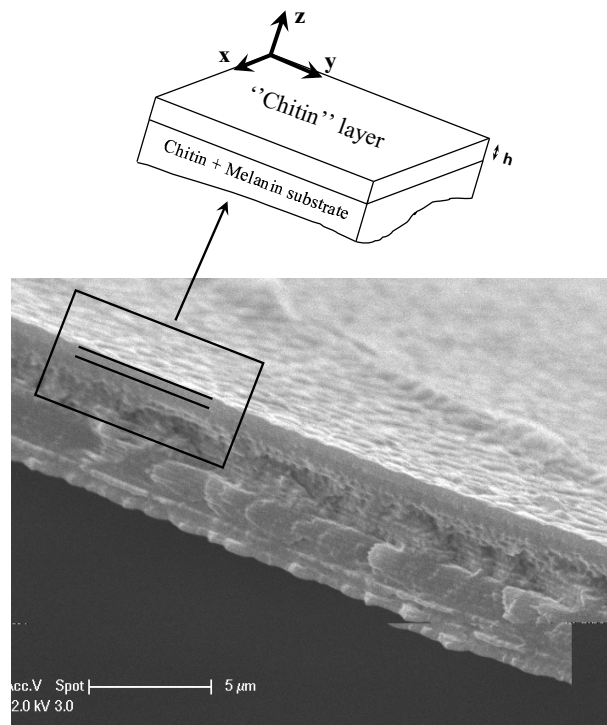


FIG. 3: *Megascolia Procer Javanensis* wing section (scanning electronic microscopy picture) and model used for simulations.

III. OPTICAL PROPERTIES OF THE WING MEMBRANE

The reflection factor of the wing membrane was measured for several incidence angles, in the specular geometry. For this purpose, a piece of wing was cut from a dry specimen and glued on a black substrate. The reflection spectra were obtained using an Avaspec 2048/2 fibre optic spectrophotometer and the reflected light was compared with a diffuse PTFE-based white reference tile. This normalization produces the “reflection factor” shown in Fig. 4. This quantity is closely related to the reflectance, which expresses the reflected power in units of the incident power. In the reflectance range of interest, due to the flat response of the white standard, these quantities differ only by a normalization factor.

The results of the measurements are given in Fig. 4, where the red curves (experimental results) describe the spectral response of a wing under varying incidences. All these measurements were performed on a forewing, in a specular geometry (with an emergence angle equal to the incidence angle, both measured from the normal to the wing surface). The incidence plane was directed along the length of the wing.

At normal incidence the backscattering measurement reveals oscillations with reflection maxima for wavelengths near 325 nm, 505 nm and 1015 nm. The broad lineshape of these reflection band is reminiscent of the single slab resonances, except for the increase of the reflection maxima. The overall effect obtained is a lack of reflected intensities between 600 and 800 nm, which basically covers the orange-red colorimetric region. This is consistent with the blue-green colouration of the wing. Smooth oscillations of the reflectance spectrum, as a function of the wavelength, indicate the interference of a small number of waves and this is consistent with the interference occurring in the thin layer and with a low refractive index contrast at the substrate interface.

When the angle of incidence is increased, the spectrum is slightly blue-shifted, as one would expect from this single slab interference mechanism. It is important to know the refractive indices in order to make more precise predictions and to build an accurate model of the wing’s optical behaviour. This is the subject of the next section.

IV. DETAILED MODELLING

Electron microscopy reveals a wing made of a stack of “mechanical” (thin and rigid) slabs covered by a biopolymer layer. The thickness of the mechanical layers varies along the wing, while the thickness of the upper surface layer is constant. On the other hand, the hue selection is constant over the whole surface of the wings, which suggests that

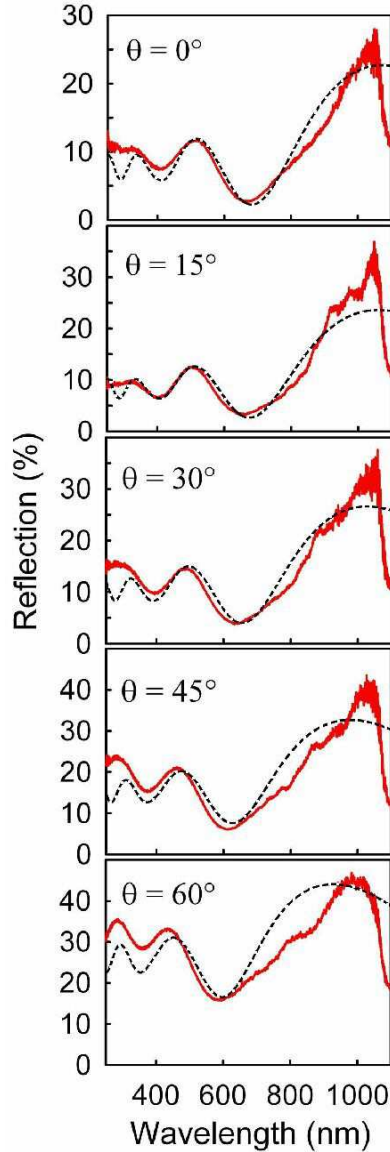


FIG. 4: (Colour online) Wings reflection as a function of the wavelength for various incidence angles. Experimental data (solid line) and simulations results (dashed line).

the stack multilayer should be considered an homogeneous and very absorbant substrate and the upper surface layer (of thickness about 300 nm), the optical filter. The upper layer is transparent, and its dielectric function is likely to be close to that of chitin (indeed, in ethanol, with a refractive index 1.4, close enough to that of chitin, the iridescence of the wasp's wing is reversibly suppressed, as Fig. 5 shows).

In the context of a single optical slab model, the reflection coefficient \mathcal{R} is given by

$$\mathcal{R} = \left| \frac{r_1 + r_2 e^{2i\beta}}{1 + r_1 r_2 e^{2i\beta}} \right|^2 \quad (1)$$

where r_1 (r_2) is the Fresnel reflection coefficient on the air/slab interface (on the slab/substrate interface), and

$$\beta = \frac{2\pi}{\lambda} h \sqrt{n_L^2 - \sin^2 i} \quad (2)$$

h is the slab thickness, n_L the refraction index of the upper layer, λ the wavelength of the incident light and i the angle of incidence. In this context, the condition for constructive interference in the reflected beam under the incidence i is

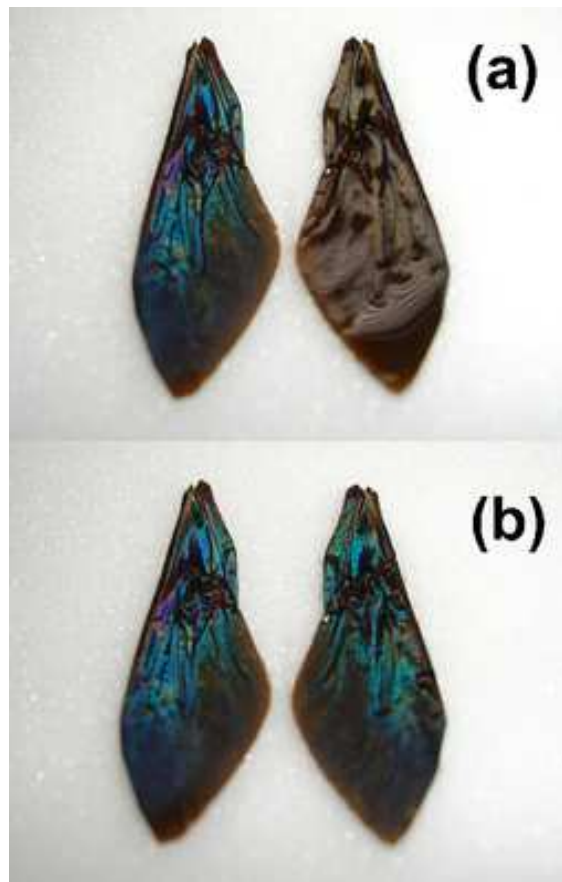


FIG. 5: (Colour online) (a) In this upper panel, the wing on the left has been kept dry as a reference, and the wing on the right is covered with a macroscopic layer of liquid ethanol (refractive index 1.4). The wet wing loses its blue-green iridescence and shows a dark-brown appearance, due to the strong attenuation of the outer interface refractive index contrast. (b) When ethanol is removed by evaporation, the wing returns to its original iridescent appearance.

that the incident wavelength verifies (see Fig. 6)

$$\lambda_{\max} = \frac{2h\sqrt{n_L^2 - \sin^2 i}}{m} \quad (3)$$

where m is a positive integer. By contrast, the condition for destructive interference in the reflected beam is that the incident wavelength verifies

$$\lambda_{\min} = \frac{4h\sqrt{n_L^2 - \sin^2 i}}{2m + 1} \quad (4)$$

The wavelengths related to the main reflection maxima or minima for many incidence i are known from experiment. Using Eqs. 3 and 4 it is then possible to fit both the overlayer thickness h and its refractive index n_L . The precise dispersion of the upper layer material remains unknown and it can be neglected in the present case. One gets $h = 286$ nm (that is in agreement with SEM assessment) and $n_L = 1.76$ (in accordance with the above hypothesis). Though the basic molecule of chitin is well defined - $(C_8H_{13}O_5N)_n$ - the full composition of the hard surfaces of arthropods is highly variable and the refractive index of the “chitinous” exoskeleton of insects and other classes of animals is not universal : values from 1.52 to as much as 2 have been reported in various studies. The melanin contents, which increases opacity, also causes an increase of the refractive index, a correlation which can be expected from Kramers-Kronig causal constraints. An average index of 1.76 gives a material which is less refractive than what we will find in the wing substrate, so that we will refer to the overlayer material as being “chitin”, emphasizing the relative lack of melanin in this layer.

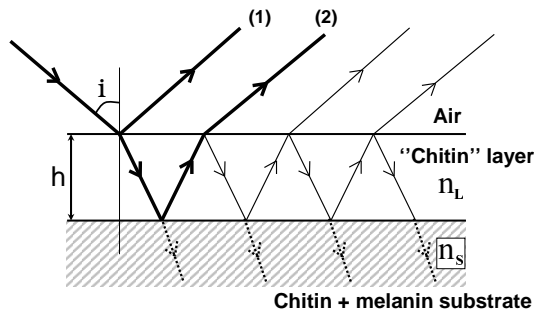


FIG. 6: Schematic representation of the wing structure, showing how the reflection takes place through the multiple paths of light.

The refractive index of the opaque melanin-loaded chitin, which makes the flexible wing substrate also calls for attention. We first note that a single slab overlayer model implies that the maxima of the reflection amplitude (neglecting absorption) reach the values

$$\mathcal{R}_{\max} = \left(\frac{r_1 + r_2}{1 + r_1 r_2} \right)^2 \quad (5)$$

whereas minima of the amplitude take the values

$$\mathcal{R}_{\min} = \left(\frac{r_1 - r_2}{1 - r_1 r_2} \right)^2 \quad (6)$$

Since r_1 must be constant (as n_L dispersion is neglected in this model), only a strong dispersion of the substrate refractive index n_S can make \mathcal{R}_{\max} and \mathcal{R}_{\min} (through r_2) vary with the wavelength λ . An experimental assessment of \mathcal{R}_{\max} and \mathcal{R}_{\min} allows to fit the real part n_S of the complex index in the following way :

$$n'_S = \begin{cases} 1.89 & \text{if } \lambda \leq 400 \text{ nm} \\ 1.45 \times 10^6 \lambda + 1.31 & \text{if } \lambda \geq 400 \text{ nm} \end{cases} \quad (7)$$

An imaginary part must also be considered, as melanin involves absorption. Following Albuquerque et al. [20], for visible wavelengths, this imaginary part will be assigned the value $n''_S \sim 0.02$. The transmission coefficient of a $5\text{-}\mu\text{m}$ thick slab with this absorption response will not exceed 21% at 800 nm and will even be smaller for shorter wavelengths.

Fig. 4 also shows the results of calculations (black curves) based on the above refractive indexes. This calculation uses a simple one-dimensional coupled-modes theory, that combines a scattering matrix formalism with a plane wave representation of the fields. This method is well known [21] and do not need a detailed description. In Fig. 4, experimental and theoretical results are shown and compared for a few specific angles of incidence (0° , 15° , 30° , 45° and 60°). The measured and computed location and line width of the reflection bands correlate satisfactorily. The thin layer model is then clearly consistent with the observed reflection factor. The location of the maxima and minima can easily be understood from a thin-film interference model. Indeed, given the progression of the refractive indexes (1 outside, n_L in the film, n_S for the substrate), constructive interference under the incidence i will occur for incident wavelengths that verify equations (3), just as destructive interference will occur for incidence wavelengths that verify equation(4) (see Fig. 6). For instance, at normal incidence, this simple formula predicts the following destructively reflected wavelengths : 671 nm, 403 nm,... These clearly agree with the spectral observations (656 nm, 404 nm,...and match spectral calculations.

The blue-shift of the maxima and minima of the reflection coefficient with the increase in the angle of incidence is well predicted. The maxima-minima damping is also well described justifying the introduced dispersion of the melanin/chitin mixture. In addition, calculated curves do not present significant differences if n''_S is set equal to zero (not shown). As a consequence, melanin absorption do not play a significant role in the present context, except for providing a dark background which makes easier perceiving the colored iridescence.

The color perceived from the reflection intensity can be described by chromaticity coordinates that can be calculated in the framework of standard human colorimetry. Fig. 7 shows the color trajectories with the D65 illuminant, in the xy CIE 1931 chromaticity standard, as a function of the angle of incidence, for both the theory and experimental reflectance curves.

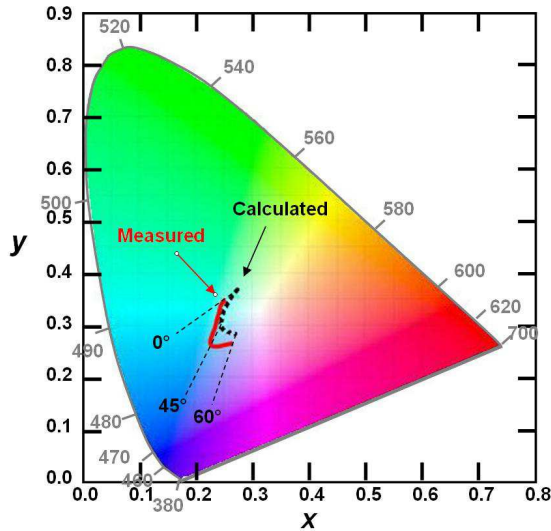


FIG. 7: (Colour online) Colorimetric trajectories for light reflected from the the wing of the wasp, for varying incidence angles, in the range from 0 to 60°. Solid line is from experimental data ; dashed line is from the model calculation.

The fine details perceived in the lineshape of the $m = 1$ reflection, near $\lambda = 1006$ nm is not properly accounted by the monolayer model. The appearance of structures on the lineshape of this interference fringe could be due to secondary interferences through the full thickness of the wing, but the fundamental would appear far in the infrared, and harmonics in the visible range should be weak, due to the strong melanin absorption. We suggest that these structures are associated with the surface roughness of the overlayer. As seen above, the wing surface presents a roughness on a typical length scale of 1200 nm and, via the decay to and from guided modes (Fano resonances) [22] this can cause diffraction and addition of spectral oscillations on the short-wavelength side of the fringe. With a 1200 nm “horizontal” grating on such structure, diffraction can change the reflected wavelength by about $\Delta\lambda \approx 100$ nm, consistent with the observed spectral location of the structure (see, for instance, on Fig. 4 the weak peak near 980 nm for $\theta = 15^\circ$). At the moment, however, theory seems unable to accurately predict the observed intensities of these fringe perturbations, so that the question - out of the scope of the present paper - should be given some further attention.

V. CONCLUSION

We have shown that the iridescence of the wings of *Megascolia Procer Javanensis* can be reasonably well understood as resulting from the interference of light in a thin optical chitin layer covering a chitin/melanin absorbing structure.

This wasp is equipped with opaque wings which contain a high concentration of melanin. The black background defined by this chitin/melanin structure allows for a particularly highly visible structural blue-green colouration, generated by an extremely simple device, using a minimal number of interfering waves : a constant-thickness overlayer covering all four wings. This is among the most elementary interference filters and, in spite of its simplicity, it turns out to be very effective. It is interesting to note that, in a very different context, evolution has produced similar structures on birds : the domestic pigeon [23], which displays some feathers with green iridescence, and others with violet iridescence, use the same strategy. In the bird, the “ active” overlayer is the cortex of the barbules.

Acknowledgments

This investigation was conducted with the support of the European NEST STREP BioPhot project, under contract no. 12915. The use of Namur Interuniversity Scientific Computing Facility (Namur-ISCF) is acknowledged. This work has also been partly supported by the European Regional Development Fund (ERDF) and the Walloon Regional Government under the “PREMIO” INTERREG IIIa project. M.R. was supported by the Belgian Fund for Industrial and Agronomic Research (FRIA). V.W. acknowledges the support of the Belgian National Fund for Scientific Research

(FNRS).

-
- [1] J. Zi, X. Yu, Y. Li, X. Hu, C. Xu, X. Wang, X. Liu, and R. Fu, Proc. Natl. Acad. Sci. USA **100**, 12576 (2003).
 - [2] J. P. Vigneron, J.-F. Colomer, M. Rassart, A. L. Ingram, and V. Lousse, Phys. Rev. E **73**, 021914 (2006).
 - [3] A. R. Parker, R. C. McPhedran, D. R. McKenzie, L. C. Botten, and N. A. Nicorovici, Nature **409**, 36 (2001).
 - [4] V. Welch, J. P. Vigneron, V. Lousse, and A. Parker, Phys. Rev. E **73**, 041916 (2006).
 - [5] A. R. Parker, V. L. Welch, D. Driver, and N. Martini, Nature **426**, 786 (2003).
 - [6] H. Ghiradella, D. Aneshansley, T. Eisner, R. E. Silberglied, and H. E. Hinton, Science **178** (4066), 1214 (1972).
 - [7] H. Tada, S. E. Mann, I. N. Miaoulis, and P. Y. Wong, Applied Optics **37** (9), 1579 (1998).
 - [8] S. Yoshioka and S. Kinoshita, Proceedings of the Royal Society of London Series B **271** (1539), 581 (2004).
 - [9] C. R. Lawrence, P. Vukusic, and R. Sambles, Applied Optics **41** (3), 437 (2002).
 - [10] P. Vukusic, J. R. Sambles, C. R. Lawrence, and R. J. Wootton, Nature **410** (6824), 36 (2002).
 - [11] A. Argyros, S. Manos, M. C. J. Large, D. R. McKenzie, G. C. Cox, and D. M. Dwarde, Micron **33** (5), 483 (2002).
 - [12] Z. Veretzky, Z. Balint, K. Kertesz, D. Mehn, I. Kiricsi, V. Lousse, J.-P. Vigneron, and L. Biro, Microscopy and Analysis **18**, 25 (2004).
 - [13] J. P. Vigneron, M. Rassart, C. Vandembem, V. Lousse, O. Deparis, L. P. Biró, D. Dedouaire, A. Cornet, and P. Defrance, Phys. Rev. E **73**, 041905 (2006).
 - [14] T. Osten, Linzer biologische Beiträge **32**(2), 537 (2000).
 - [15] J.-H. Fabre, *Souvenirs entomologiques, 3rd series* (Ed. Ch. Delagrave, Paris, 1891).
 - [16] N. Vereecken and J. Carriere, Notes fauniques de Gembloux **53**, 71 (2003).
 - [17] J. G. Betrem and J. C. Bradley, Zool. Meded. **39**, 433 (1964).
 - [18] J. G. Betrem and J. C. Bradley, Zool. Meded. **40**, 89 (1964).
 - [19] I. Hooper, P. Vukusic, and R. Wootton, Optics Express **14**, 4891 (2006).
 - [20] J. de Albuquerque, C. Giacomantonio, A. White, and P. Meredith, Eur. Biophys. J. **35**, 190 (2006).
 - [21] J. P. Vigneron and V. Lousse, Proc. SPIE **6128**, 61281G (2006).
 - [22] M. Sarrazin, J.-P. Vigneron, and J.-M. Vigoureux, Phys. Rev. B **67**, 085415 (2003).
 - [23] H. Yin, L. Shi, J. Sha, Y. Li, Y. Qin, B. Dong, S. Meyer, X. Liu, L. Zhao, and J. Zi, Phys. Rev. E **74**, 051916 (2006).